JOURNAL OF CATALYSIS **178,** 450–456 (1998)
ARTICLE NO. CA982121

Effects of Particle Size on the Progressive Oxidation of Nanometer Platinum by Dioxygen

Chen-Bin Wang and Chuin-Tih Yeh[1]

Department of Chemistry, National Tsinghua University, Hsinchu, Taiwan 30043, Republic of China

Received September 9, 1997; revised April 22, 1998; accepted April 28, 1998

Platinum particles in nanometer size were dispersed on the γ-Al_2O_3 support by the impregnation technique. Oxidation phenomena of the supported particles with dioxygen were pursued by a simultaneous TG-DSC technique. Observed extent of oxidation varies in four consecutive steps, i.e., adsorption of oxygen on the surface of supported platinum crystallites at ambient or lower temperatures, reconstruction of platinum surface for extended accommodation of oxygen above 300 K, formation of a stable surface layer of platinum oxides about 750 K, and desorption of oxygen and/or platinum dioxide over 800 K, while raising the temperature. Measured heat of oxidation ($-Q_{ox}$) generally decreases with the extent of oxidation. The particle size (d) of dispersed platinum has a profound effect on the oxidation. The species of surface platinum oxide formed at 770 K was Pt^sO_2 [$-\Delta H_f = 190$ kJ (mol O_2)$^{-1}$] as $d < 1.3$ nm but became Pt^sO [$-\Delta H_f = 169$ kJ (mol O_2)$^{-1}$] on $d > 2.0$ nm. The heat of dioxygen adsorption (ΔH_{ad}) at $T < 300$ K could be also correlated with the average diameter (d) of supported platinum according to $-\Delta H_{ad}$ [kJ (mol O_2)$^{-1}$] $= 406 - 81\ d$/nm when the platinum diameter was less than 2.5 nm.

INTRODUCTION

Alumina-supported platinum is widely used for catalyzing many oxidation reactions, such as the VOC combustion and the abatement of motor vehicle emissions. The mechanism of these oxidation reactions involves inevitably an oxidation of the supported platinum into platinum oxide and a reduction of the platinum oxides (by hydrocarbon or CO) back to platinum, i.e.,

$$Pt^s \leftrightarrow Pt^sO_x, \qquad [1]$$

where x denotes an adsorption stoichiometry of oxygen on platinum atoms exposed on the surface (Pt^s) of dispersed platinum crystallites. A detailed understanding of the interaction of platinum with dioxygen should be helpful towards improvements of the oxidation reactions.

Interactions of dioxygen with crystalline platinum have been extensively studied using thermal desorption spectroscopy (1–5). These studies suggested that the oxidation was limited to the surface layer of single crystals at $T < 800$ K. The following oxygen species have been distinguished from these desorption studies:

1. Molecularly adsorbed dioxygen (the α-state): this weakly adsorbed species was formed upon interactions at $T < 120$ K. But they became unstable and desorbed from the platinum surface on raising the system temperature above 160 K;
2. Atomically adsorbed oxygen (the β-state): this species became the main adsorbate upon interactions at $T > 160$ K. The desorption of this strongly adsorbed species from the platinum surface occurred at $T > 650$ K; and
3. Subsurface oxide: this species was formed through penetration of atomically adsorbed oxygen into the subsurface region of platinum crystallines at $T > 800$ K. The penetrated oxygen anions desorbed at $T > 1250$ K.

Both the heat of dioxygen adsorption (ΔH_{ad}) on platinum surface and the enthalpy of platinum oxide formation (ΔH_f) have been extensively pursued in the literature (1, 2, 4, 6–22). Reported ΔH_{ad} and ΔH_f scattered from 301 to 119 kJ (mol O_2)$^{-1}$ (see Table 1 (1, 2, 4, 6–18)) and from 222 to 134 kJ (mol O_2)$^{-1}$ (see Table 2 (15, 19–22)), respectively, for different samples of platinum.

In previous papers (23, 24), we have studied the interaction of Pd/Al_2O_3 and Rh/Al_2O_3 with dioxygen using the TG-DSC technique. Both the ΔH_{ad} and the ΔH_f of these interactions were found to vary, to a different extent, with the particle size of the crystallites. In this study, we want to demonstrate that the literature variations in ΔH_{ad} and ΔH_f of platinum–dioxygen interaction also can be attributed mainly to differences in the size of platinum crystallites.

EXPERIMENTAL

Sample Preparation

Platinum catalysts of various platinum loadings were prepared by impregnating γ-Al_2O_3 (Merck, surface area = 108 m^2/g) with different amounts of an aqueous H_2PtCl_4 solution. Obtained slurries were pretreated sequentially

[1] To whom correspondence should be addressed. E-mail: ctyeh@chem.nthu.edu.tw.

0021-9517/98 $25.00

TABLE 1

Heat of Dioxygen Adsorption on Platinum Reported in Previous Literature

Sample	Technique	$-\Delta H_{ad}$/kJ (mol O_2)$^{-1}$	Reference
Pt(100)	TPD	119	(6)
Pt(100)	TPD	$\beta_2 = 160$	(7)
Pt(100)	TPD	($\beta_1 = 192$, $\beta_2 = 161$)	(8)
Pt(100)	TPD	($\beta_3 = 290$, $\beta_2 = 260$, $\beta_1 = 187$)	(9)
Pt(111)	TPD	$\beta = 190$, $\alpha = 37$	(4)
Pt polycrystalline	TPD	($\beta = 167$, $\alpha = 146$)	(2)
Pt polycrystalline	TPD	($\beta = 184$, 159)	(10)
Pt filament	TPD	($\beta_4 = 226$, $\beta_2 = 163$, $\alpha = 25$)	(1)
Pt filament	TPD	242	(11)
Pt filament	Isosteres	$217 \rightarrow 176$[a]	(12)
Pt black	Calorimetry	$215 \rightarrow 118$[a]	(13)
Pt powder	Calorimetry	220 ± 25	(14)
Pt film	Calorimetry	280, 259	(15)
Pt/Al_2O_3	Calorimetry	242	(16)
Pt/Al_2O_3	Calorimetry	280, 250	(17)
Pt/SiO_2	Calorimetry	284 ± 37	(14)
Pt/TiO_2	Calorimetry	301	(18)

[a] The range indicates that the differential enthalpy decreases with the coverage (θ).

with an overnight drying at 380 K, a 4-h calcination at 770 K, a 1-h reduction by flowing hydrogen at a temperature (T_r) of 670 K (to convert the PtO_nCl_m to Pt crystallites (25)) or higher temperatures (to sinter the supported Pt). Platinum loadings on the reduced samples were determined by the atomic-emission technique using an ICP-MS (Perkin-Elmer). The dispersion (D) of platinum on reduced samples was volumetrically determined by dihydrogen chemisorptions at 300 K on assuming a N_H^m/N_{Pt^s} stoichiometry of 1.1 (26, 27) at the monolayer adsorption. The third column of Table 3 lists dispersions estimated for the prepared samples. We found that the estimated dispersion of a 4.13% Pt/Al_2O_3 sample generally decreased with the reduction pretreatment upon $T_r > 800$ K. However, the average diameter of sintered platinum remained less than 2.2 nm.

TABLE 2

Heat of Formation Reported in Previous Literature for Various Bulk Platinum Oxides

Author	Method	Platinum oxides	$-\Delta H_f$/kJ (mol O_2)$^{-1}$	Reference
Tagirov *et al.*	C–C equation[a]	PtO_2	222	(19)
Latimer	Electrochemical	PtO_2	167 ± 42	(20)
Brennan *et al.*	Calorimetric	PtO	142	(15)
Brewer		PtO	142 ± 42	(21)
		Pt_3O_4	134 ± 50	
		PtO_2	134 ± 42	
CRC data		Pt_3O_4	163	(22)

[a] Calculated by Clausius–Clapeyron equation.

Simultaneous Gravimetric and Calorimetric Measurements

The oxidation of reduced samples by dioxygen was carried out in a dual port calorimeter (Setaram TG-DSC 111). This instrument permits evacuation treatments under a vacuum pressure of 2×10^{-1} Torr as well as simultaneous TG (thermogravimetry) and DSC (differential scanning calorimetry) measurements in a temperature range between the ambient temperature, 280 K, and 970 K. The sensitivity of the TG and the DSC was 0.25 μg and 10 μw, respectively. Pure Al_2O_3 was mounted in the reference port of the calorimeter as a blank to offset possible changes (Δm and ΔH) caused by the support.

While raising the system temperature from RT to 670 K at a rate of 10 K/min, each testing sample was purged in the calorimeter with a flow of Ar (30 ml/min, around 1 bar pressure). After the temperature reached 670 K, a 1-h pulse of 10 ml/min hydrogen was added from an auxiliary inlet into the Ar flow to reduce the sample. After terminating the hydrogen pulse, the sample temperature was subsequently raised further to 720 K to desorb the adsorbed hydrogen. The reduced sample was cooled in the Ar flow to a predetermined oxidizing temperature (T_{ox}) and then oxidized by a flow of 10 ml/min dioxygen introduced from the auxiliary inlet into the Ar flow. The oxidation phenomena were examined by the calorimeter through a gain in weight (Δm_{ox}) as well as a simultaneous evolution of heat (q_{ox}).

Figure 1 presents a time profile of TG-DSC measurement on oxidizing 36.4 mg of the 4.13% Pt/Al_2O_3 sample with dioxygen at 300 K. The measurement indicated that the oxidation was an exothermic reaction accompanied with a gain in weight. The rate of oxidation was fast at the initial stage, but decreased gradually with the reaction time. After 2×10^3 s of oxidation, a $\Delta m = 74.3$ μg and a $q_{ox} = -0.705$ J were obtained. The oxygen uptake, N_O, in each experiment was determined, tentatively, from the Δm_{ox} obtained upon 2×10^3 s of oxidation.

RESULTS AND DISCUSSION

Gravimetric Measurements

The uptake of dioxygen by each Pt/Al_2O_3 sample upon an oxidation of 2×10^3 s varied with the oxidation temperature. Figure 2 compares temperature profiles of oxygen uptake (in terms N_O/N_{Pt^s}, where N_{Pt^s} denotes the number of Pt atoms exposed to surface) observed on three reduced samples. In this uptake study, a fresh sample was used in each data point. On raising the oxidation temperature from 280 to 900 K, each observed profile can be distinguished into following four stages:

TABLE 3

Heats of O_2 Adsorption and Enthalpy of Pt^sO_x Formation on Pt/Al_2O_3

Sample	T_{red}/K	Hydrogen chemisorption		Oxygen adsorption		Formation of surface oxide		
		D (N_H^m/N_{Pt})	d (nm)	N_O^{ad}/N_{Pt^s}	$-Q_{ad}$/kJ (mol O_2)$^{-1}$	N_O^*/N_{Pt^s}	$-\Delta H_f$/kJ (mol O_2)$^{-1}$	Possible Pt^sO_x
0.8% Pt	670	1.00	1.0	1.01	329	2.04	193	Pt^sO_2
2.1% Pt	670	1.02	1.0	1.02	328	1.98	189	Pt^sO_2
4.1% Pt	670	0.80	1.3	0.60	303	1.89	186	Pt^sO_2
	770	0.87	1.2	0.68	313	1.52	184	Pt^sO_2 & Pt^sO
	820	0.68	1.5	0.49	282	1.50	181	Pt^sO_2 & Pt^sO
	870	0.63	1.6	0.38	270	0.89	166	Pt^sO
	920	0.56	1.8	0.31	264	0.95	169	Pt^sO
	950	0.48	2.1	0.12	240	1.12	170	Pt^sO
	970	0.45	2.2	0.10	230	1.10	171	Pt^sO

Note. N_H^m: Monolayer uptake of hydrogen atom from H_2 chemisorption at 300 K. Assuming that $N_H^m/N_{Pt} = 1.1$. d: Average diameter of platinum crystallites calculated from $1.0/(N_H^m/N_{Pt})$. N_O^{ad}: Uptake of oxygen atom at 300 K. N_O^*: Uptake of oxygen atom at 770 K.

(a) The N_O/N_{Pt^s} ratio remained at a base value at $T < 300$ K;

(b) The ratio gradually increased from the base value to a plateau value in the temperature range between 300 and 720 K;

(c) The ratio stayed at the plateau value at temperatures around 750 K; and

(d) The ratio decreased sharply upon $T > 800$ K.

In an isobaric (100 Torr O_2) measurement, Ho (28) found that the extent of oxygen uptake by platinum black was constant in the temperature range between 200 and 300 K, but increased substantially on raising the oxidation temperature above 300 K. The constant uptake at $T < 300$ K was attributed to an adsorption of oxygen on the surface of platinum crystallites. Accordingly, the oxygen uptake found in stage (a) of Fig. 2 is also regarded, in this report, as the chemisorption of oxygen on the platinum surface. Helms *et al.* (29) suggested that the O_2 chemisorption on platinum is a structure-sensitive reaction. Maire *et al.* (30) also found, from Auger electron spectroscopy, that different planes of a platinum crystal exhibit different activities toward oxygen. The fifth column of Table 3 indicates that the N_O^{ad}/N_{Pt^s}

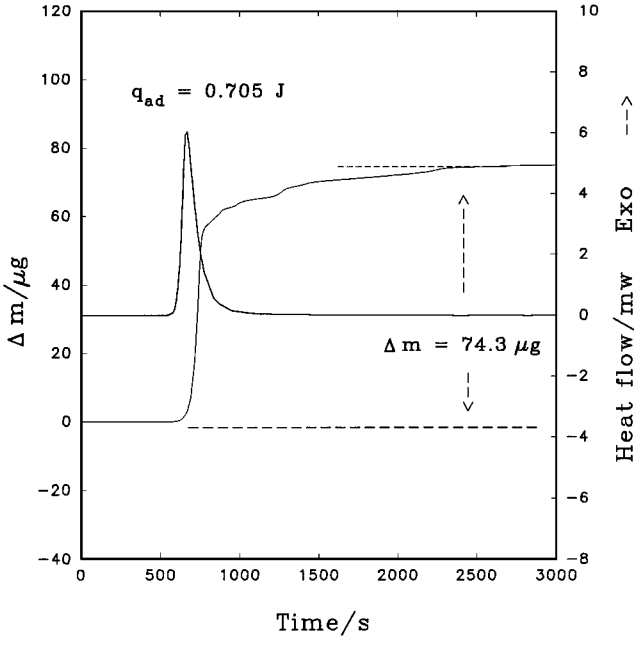

FIG. 1. The TG-DSC diagram obtained from oxidation of 36.4 mg 4.13% Pt/Al_2O_3 sample with dioxygen at 300 K. An oxygen uptake of 74.3 μg and a simultaneous evolved heat of 0.705 J was obtained after 2×10^3 s of oxidation.

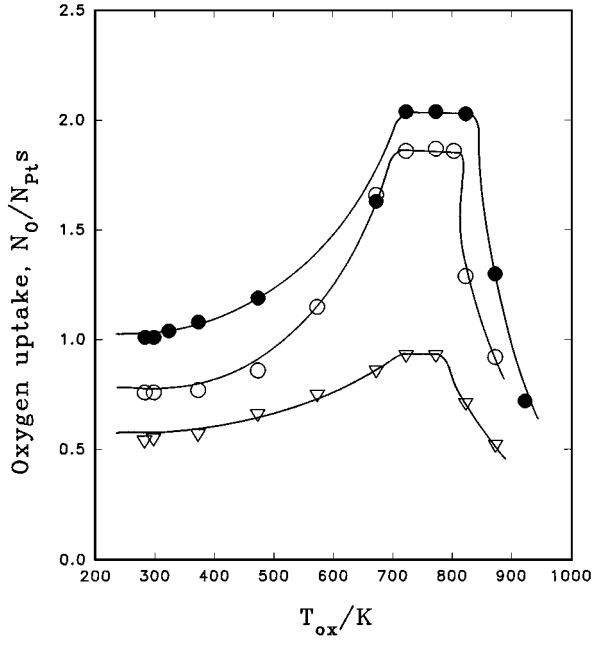

FIG. 2. Temperature profiles of dioxygen uptake on the surface of three Pt/Al_2O_3 samples: (a) 0.83% Pt, prereduced at 670 K, D = 100% (●); (b) 4.13% Pt, prereduced at 670 K, D = 80% (○); (c) 4.13% Pt, prereduced at 920 K, D = 56% (▽).

stoichiometry of the chemisorption-stage (uptake of oxygen atom at 300 K) definitely increased with an increase in the dispersion of platinum. The same conclusion has already been reached in the literature for other platinum samples (9).

The oxide ions chemisorbed on platinum crystallites may induce a surface reconstruction (31, 32). Based on LEED results, Barteau *et al.* (8), Kneringer *et al.* (9), and Bonzel *et al.* (33) suggested that the top layer of Pt(100) surface reconstructed in an oxygen environment upon $T > 300$ K. Such reconstruction produced a buckled surface or microfacets that can promote an increment in oxygen uptakes. Nevertheless, the penetration of atomically oxygen ions into the subsurface of platinum crystallites occurred only at $T > 800$ K. Savchenko (34) proposed, from XPS and TPD studies of oxygen adsorption on platinum surfaces, that adsorbed oxygen atoms might insert, at $T < 700$ K, into subsurface platinum layers located at open planes [(100), (112), and (210)] to form "surface oxides." Paryjczak *et al.* (35) and McCabe *et al.* (36) studied the interaction of supported crystallites of platinum (such as Pt/Al_2O_3) with dioxygen using pulse gas chromatographic method. Their results also found that the oxidations preserved superficial characters upon $T_{ox} < 900$ K. Accordingly, the increasing N_O/N_{Pt^s} ratio found in stage (b) of Fig. 2 is assigned to an incremental accommodation of oxygen during the reconstruction of the platinum surface. The confinement of surface oxidation implies not only that the migration of adsorbed oxide ions into subsurface layers of platinum has a potential barrier, but that the thermal agitation at $T < 300$ K is insufficient to overcome the barrier.

According to the results of Fig. 2, we can understand that the extent of surface oxidation (N_O/N_{Pt^s} ratio) depends heavily on the oxidation temperature and particle size of the platinum samples. A plateau ratio was attained for each sample when the oxidation temperature was raised over 700 K in stage (c) of Fig. 2. This plateau is assigned to a formation of surface oxide (Pt^sO_x) structure. The seventh column of Table 3 lists calculated N_O/N_{Pt^s} ratios at the plateau and the ninth column presents the species of surface oxides expected from the ratios. The plateau ratio stayed around 2.0 (indicating a stoichiometry of Pt^sO_2) for highly dispersed samples ($D > 80\%$), but gradually decreased to 1.0 (Pt^sO) on decreasing the dispersion.

A formation of different surface oxides, i.e., Pt^sO_2 (25, 37, 38), $Pt^sO_{1.33}$ (39), and Pt^sO (40) has been reported in the literature on oxidations of platinum crystallites. Our results demonstrated that the N_O/N_{Pt^s} stoichiometry of stable oxides formed on the surface of platinum crystallites definitely increased with the dispersion of platinum. Species of Pt^sO_2 or Pt^sO was formed on samples at $D > 80\%$ or $D < 60\%$, respectively.

The filamental platinum is widely employed to promote the ammonia oxidation and the synthesis of hydrogen cyanide. A loss of platinum generally occurs upon operations at higher temperatures ($T > 700$ K) and is attributed to desorptions of gaseous $PtO_2(g)$ (41–45) from the filaments, i.e.,

$$Pt^s + O_2 \rightarrow PtO_2(g). \quad [2]$$

Platinum oxides formed at the surface of platinum may also desorb O_2 at higher temperatures (650–1250 K) (1, 4, 7–9, 21) through

$$Pt^sO_x \rightarrow Pt^s + x/2\ O_2. \quad [3]$$

The weight loss found in the stage (d) of Fig. 2 may therefore be attributed to the sublimation of PtO_2 (reaction [2]) as well as the oxygen desorption (reaction [3]). In order to assess the competition of these two reactions, we analyzed the loading of platinum that remained in samples after each oxidation treatment using the atomice mission technique (samples were digested with a 1 : 3 HF-aqua regia solution). Figure 3 shows fractions of platinum lost at different oxidation temperatures. The observed loss at $T = 870$ K was insignificant for highly dispersed samples but became substantial on decreasing the platinum dispersion. The low volatility of PtO_2 on the highly dispersed samples may be caused by a strong adhesive interaction between the alumina surface and supported platinum atoms. Accordingly, the sharp decrease of N_O/N_{Pt^s} ratio in stage (d) may be attributed mainly to the desorption of oxygen (reaction [3]) for the 100% dispersed sample. For lowly dispersed ($D < 100\%$) samples, however, sublimation of

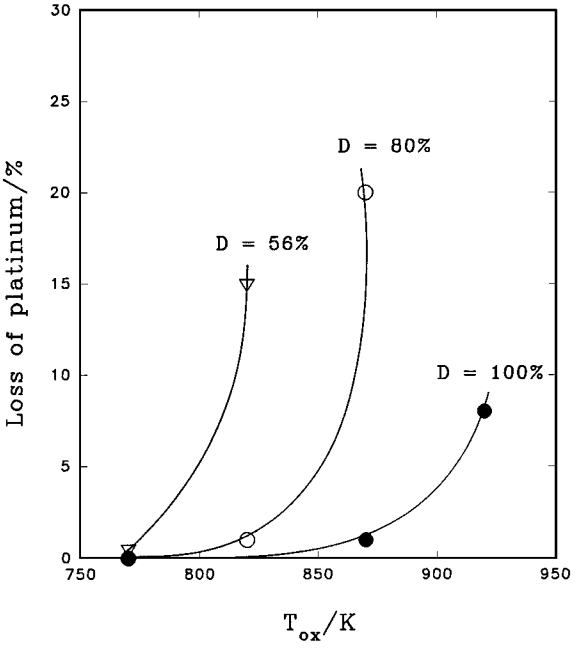

FIG. 3. Variations in the loss of platinum from Pt/Al_2O_3 samples of different dispersions with oxidation temperature.

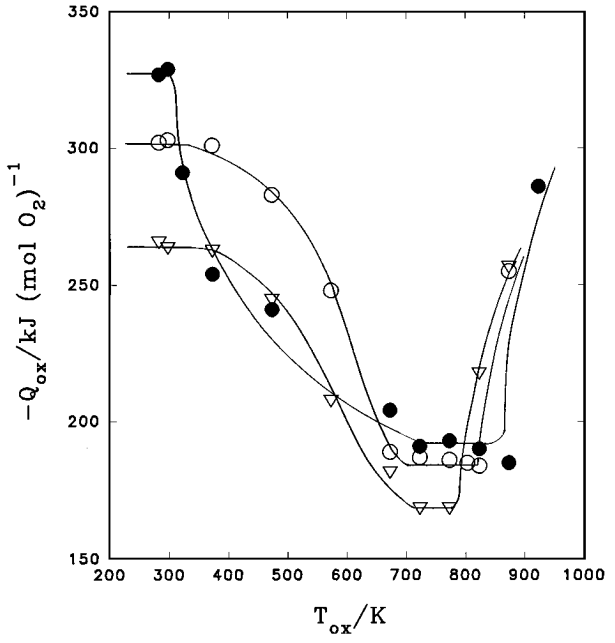

FIG. 4. Temperature profiles of heat of oxidation (Q_{ox}) from samples of: (a) 0.83% Pt, prereduced at 670 K, D = 100% (●); (b) 4.13% Pt, prereduced at 670 K, D = 80% (○); (c) 4.13% Pt, prereduced at 920 K, D = 56% (▽).

platinum oxide (reaction [2]) competes with the desorption for the weight loss observed in stage (d).

Calorimetric Measurements

Figure 4 compares the temperature profiles of heat evolution ($-Q_{ox}$) upon oxidation of the 0.83% and the 4.13% Pt/Al_2O_3. The observed heat varied with both the dispersion of platinum and the oxidation temperature. Incidentally, the four oxidation stages described in the gravimetric measurements appeared again in the temperature profiles of this figure: the heat of oxidation displayed a plateau value at the chemisorption stage (when $T < 300$ K); it gradually decreased to a bottom value on the surface oxidation stage; it remained at the bottom value around 700 K; and it abruptly increased at the decomposition (and/or the vaporization) stage (upon $T > 800$ K). The plateau value was the heat of oxygen adsorption ($-\Delta H_{ad}$) while the bottom value may be considered as the enthalpy of platinum-oxide formation [$-\Delta H_f(Pt^sO_x)$]. Although the obtained ΔH_{ad} and ΔH_f varied with the size of the platinum crystallites, the heat evolved in each sample decreased generally with the ratio of N_O/N_{Pt}.

As is noted in Table 1, platinum crystallites with a large particle size (in samples of single crystals (4, 6–9), polycrystallines (2, 10), filaments (1, 11, 12), and powders (14)) generally have lower ΔH_{ad} values (~190 kJ (mol O_2)$^{-1}$) than those (~280 kJ (mol O_2)$^{-1}$) with a small size (in supported samples (14, 17, 18)). However, "whether ΔH_{ad} for adsorption of dioxygen on supported nanometer-platinum crystallites varies with the size of platinum" remains controversial in the literature (14, 15, 17). Figure 5 correlates the results of $-\Delta H_{ad}$ measured from the TG-DSC of this study with the average diameter (d) of platinum crystallites determined from the hydrogen chemisorption. An obvious size-dependent relation is found from our samples:

$$-\Delta H_{ad}\ [\text{kJ(mol } O_2)^{-1}] = 406 - 81\ \text{d/nm}. \qquad [4]$$

The evolved heat of adsorption increased about 100 kJ (mol O_2)$^{-1}$ as the size of the platinum crystallites was decreased from 2.2 to 1.0 nm. A similar size effect on ΔH_{ad} has also been found in our previous studies on adsorptions of dioxygen on catalysts of Pd/Al_2O_3 (23) and Rh/Al_2O_3 (24).

The eighth column of Table 3 presents the $-\Delta H_f$ of Pt^sO_x on oxidation of various Pt/Al_2O_3 samples at 770 K. Measured $-\Delta H_f$ values apparently varied with the stoichiometry (x) of Pt^sO_x formed. Figure 6 displayed that the obtained $-\Delta H_f$ can be correlated with the stoichiometry as

$$-\Delta H_f\ [\text{kJ(mol } O_2)^{-1}] = 147 + 22x. \qquad [5]$$

The evolved heat of surface oxide formation increased about 20 kJ (mol O_2)$^{-1}$ as the stoichiometry x was increased from 1.0 to 2.0. Our ΔH_f values are slightly higher than those (~140 kJ (mol O_2)$^{-1}$) in the previous literature for samples of bulk platinum oxides (15, 19–22) (see Table 2), but they matched well with values on the thermodynamic properties of surface platinum oxides (39, 40,

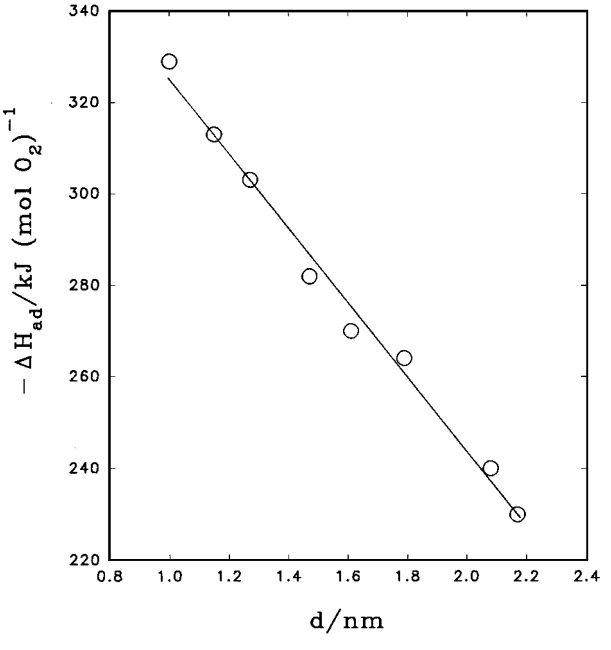

FIG. 5. Variations of ΔH_{ad} for dioxygen adsorption with the average diameter of platinum crystallites.

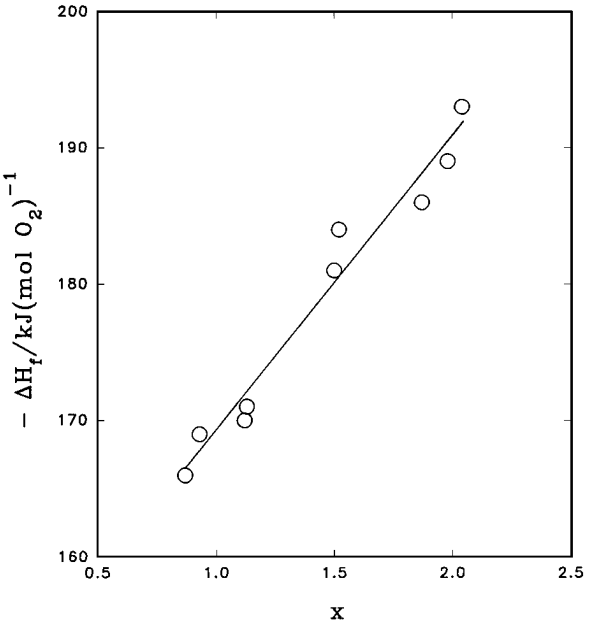

FIG. 6. Dependence of ΔH_f (Pt^sO_x) of surface platinum oxides with the stoichiometric *x*.

46, 47). Vayenas *et al.* (40, 46, 47) found from a study of solid electrolyte potentiometry that the $-\Delta H_f$ of Pt^sO_x was 188 kJ/mol O_2 for oxygen adsorbed on Pt film. Berry (39) used a high precision electrical resistance technique and found that the $-\Delta H_f$ of Pt^sO_x was 175 kJ/mol O_2 for surface oxidation of Pt wire. We believe that the difference between these two measurements comes from a slight variation in the stoichiometry of Pt^sO_x.

A Comparison of Platinum Group Metals (Pt, Pd, and Rh)

Platinum, palladium, and rhodium are three active ingredients in the catalysts of catalytic converters. Figure 7 compares the temperature profiles of the dioxygen uptake obtained in our laboratory (23, 24) on oxidation of 4.72% Pd/Al_2O_3 ($D = 21\%$), 3.26% Rh/Al_2O_3 ($D = 55\%$), and 4.13% Pt/Al_2O_3 ($D = 56\%$). Observed profiles from these three samples have a similar temperature trend. Oxygen uptakes at room temperature are low and confined to the surface adsorption, increased gradually on raising the oxidation temperature above 300 K, and reached a plateau value for $T > 700$ K. For Pd/Al_2O_3 and Rh/Al_2O_3 samples, the excessive oxidation for $T > 300$ K induced a formation of bulk oxides. In the case of Pt/Al_2O_3, however, the oxidation preserved only a superficial character by formations of a protective layer of surface oxide. Instead of penetrating into sublayers, the surface oxygen started to desorb from Pt^sO_x at $T > 800$ K.

According to the Cabrera–Mott theory (48), the magnitude of the surface-incorporation barrier (E_B) of the oxygen has a profound effect on the transition from chemisorption to bulk oxidations (49, 50). A low E_B value generally permits an easy incorporation of oxide ions into the sublayers of metal crystal to form bulk oxide. Our results therefore suggested that elements in the third transition metal series (Pt) probably have a higher E_B than the metals in the second transition metals series (Pd and Rh).

CONCLUSIONS

Oxidations of nanometer-crystallites of platinum dispersed on alumina with dioxygen were studied with a commercial TG-DSC simultaneous system. Based on the results obtained, we can conclude the following:

1. On raising the system temperature, the oxidation proceeds in four consecutive steps, i.e., surface adsorption ($T < 300$ K), reconstruction of surface to accommodate oxygen extensively ($T > 300$ K), formation of a surface layer of platinum oxides (around 750 K), and desorption of oxygen and/or platinum dioxide ($T > 800$ K).
2. Heat of oxidation for each sample decreases with an increase in the extent of oxidation.
3. Heat of the surface adsorption decreases with an increase in the size of platinum crystallites and exhibits an empirical relation of

$$-\Delta H_{ad}\ [kJ(mol\ O_2)^{-1}] = 406 - 81\,d/nm$$

when the platinum diameter is less than 2.5 nm.

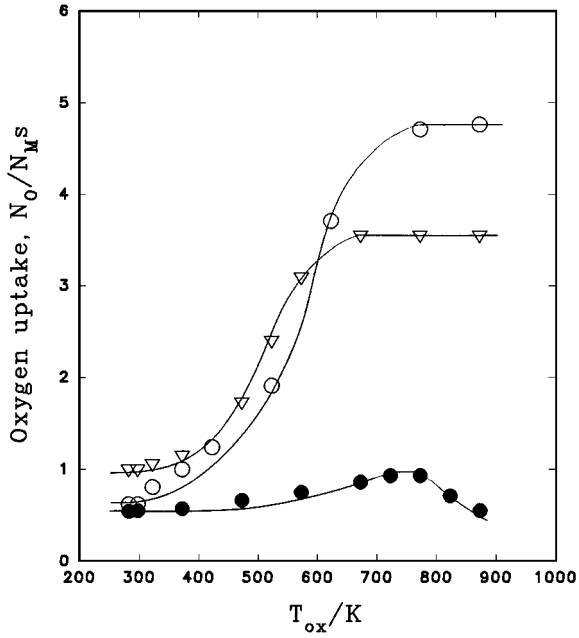

FIG. 7. Temperature profiles of dioxygen uptake on surface of various alumina supported metallic catalysts: (a) 4.13% Pt, prereduced at 920 K, D = 56% (●); (b) 4.72% Pd, prereduced at 570 K, D = 21% (○); (c) 3.26% Rh, prereduced at 670 K, D = 55% (▽).

4. Chemical stoichiometry of surface oxides (Pt^sO_x) formed at 770 K varies also with the size of platinum crystallites. The x value was 2.0 as $d < 1.3$ nm but became 1.0 as $d > 2.0$ nm.

ACKNOWLEDGMENT

The authors acknowledge the financial support of this study by the National Science Council of the Republic of China.

REFERENCES

1. Peng, Y. K., and Dawson, P. T., *Canad. J. Chem*. **52**, 3507 (1974).
2. Collins, D. M., Lee, J. B., and Spicer, W. E., *Surf. Sci.* **55**, 389 (1976).
3. Gland, J. L., and Korchak, V. N., *Surf. Sci.* **75**, 733 (1978).
4. Gland, J. L., Sexton, B. A., and Fisher, G. B., *Surf. Sci.* **95**, 587 (1980).
5. Griffiths, K., Jackman, T. E., Davies, J. A., and Norton, P. R., *Surf. Sci.* **138**, 113 (1984).
6. Derry, G. N., and Ross, P. N., *Surf. Sci.* **140**, 165 (1984).
7. Norton, P. R., Griffiths, K., and Bindner, P. E., *Surf. Sci.* **138**, 125 (1984).
8. Barteau, M. A., Ko, E. I., and Madix, R. J., *Surf. Sci.* **102**, 99 (1981).
9. Kneringer, G., and Netzer, F. P., *Surf. Sci.* **49**, 125 (1975).
10. Nishiyama, Y., and Wise, H., *J. Catal.* **32**, 50 (1974).
11. Weber, B., Fusy, J., and Cassuto, A., *J. Chim. Phys.* **66**, 708 (1969).
12. Weber, B., Fusy, J., and Cassuto, A., *J. Chim. Phys.* **71**, 1551 (1974).
13. Taylor, G. B., Kistiakowsky, G. B., and Perry, J. H., *J. Phys. Chem*. **34**, 799 (1930).
14. Sen, B., and Vannice, M. A., *J. Catal.* **129**, 31 (1991).
15. Brennan, D., Hayward, D. O., and Trapnell, B. M. W., *Proc. Roy. Soc. Ser. A* **256**, 81 (1960).
16. Basset, J. M., Theolier, A., Primet, M., and Prettre, M., *in* "5th Int. Congr. Catal., Vol. 2, 1972," p. 915.
17. Briot, P., Auroux, A., Jones, D., and Primet, M., *Appl. Catal.* **59**, 141 (1990).
18. Herrmann, J. M., Gravelle-Rumeau-Maillot, M., and Gravelle, P. C., *J. Catal.* **104**, 136 (1987).
19. Tagirov, V. K., Chizhikov, D. M., Kazenas, E. K., and Shubochkin, L. K., *Zh. Neorg. Khim*. **21**, 2565 (1976).
20. Latimer, W. M., "Oxidation Potentials," Prentice–Hall, New York, 1952.
21. Brewer, L., *Chem. Rev.* **52**, 1 (1953).
22. Lide, D. R., "Handbook of Chemistry and Physics," 72nd ed., Franklin, Bloomfield Hills, MI, 1991–1992.
23. Ho, Y. S., Wang, C. B., and Yeh, C. T., *J. Mol. Catal. A* **112**, 287 (1996).
24. Wang, C. B., and Yeh, C. T., *J. Mol. Catal. A* **120**, 179 (1997).
25. Lieske, H., Lietz, G., Spindler, H., and Volter, J., *J. Catal.* **81**, 8 (1983). [Hwang, C. P., and Yeh, C. T., *J. Mol. Catal. A* **112**, 274 (1996)]
26. O'rear, D. J., Loffler, D. G., and Boudart, M., *J. Catal.* **121**, 131 (1990).
27. Masayoshi, K., Yasunobn, I., Nobuo, T., Robert, L. B., John, B. B., and Jerome, B. C., *J. Catal.* **64**, 74 (1980).
28. Ho, Y. S., Ph. D. thesis, National Tsinghua University, 1990.
29. Helms, C. R., Bonzel, H. P., and Kelemen, S., *J. Chem. Phys.* **65**, 1773 (1976).
30. Maire, G., Legare, P., and Lindauer, G., *Surf. Sci.* **80**, 238 (1979).
31. Jona, F., *J. Phys. C: Solid State Phys.* **11**, 4271 (1978).
32. Vanselow, R., and Howe, R., "Chemistry and Physics of Solid Surfaces 5," Springer-Verlag, Berlin, 1984.
33. Bonzel, H. P., and Ku, R., *Surf. Sci.* **40**, 85 (1973).
34. Savchenko, V. I., *Kinet. Catal.* **34**, 108 (1993).
35. Paryjczak, T., Jozwiak, W. K., and Goralski, J., *J. Chromatogr.* **152**, 375 (1978).
36. McCabe, R. W., Wong, C., and Woo, H. S., *J. Catal.* **114**, 354 (1988).
37. Mills, G. A., Wellers, S. W., and Cornelius, E. B., "2nd Actes Congr. Catal., 1960."
38. Berry, R. J., *Surf. Sci.* **76**, 415 (1978).
39. Ariya, S. M., Morozova, M. P., Markevich, G. S., and Reikhardt, A. A., *J. Appl. Chem*. **23**, 1455 (1953).
40. Vayenas, C. G., and Michaels, J. N., *Surf. Sci.* **120**, L405 (1982).
41. Nowak, E. J., *J. Chem. Eng. Sci.* **24**, 421 (1969).
42. Satterfield, C. N., "Heterogeneous Catalysis in Industrial Practice," McGraw–Hill, New York, 1991.
43. Alcock, C. B., and Hooper, G. N., *Proc. Roy. Soc. A* **254**, 551 (1960).
44. Chaston, J. C., *Platinum Metals Rev.* **8**, 50 (1964).
45. Krier, C. A., and Jaffee, R. I., *J. Less-Common Metals.* **5**, 411 (1963).
46. Vayenas, C. G., Lee, B., and Michaels, J., *J. Catal.* **66**, 36 (1980).
47. Vayenas, C. G., Georgakis, C., Michaels, J., and Tormo, J., *J. Catal.* **67**, 348 (1981).
48. Cabrera, N., and Mott, N. F., *Rep. Prog. Phys.* **12**, 163 (1948).
49. Ronay, M., and Nordlander, P., *Phys. Rev. B* **35**, 9403 (1987).
50. Nordlander, P., and Ronaty, M., *Phys. Rev. B* **36**, 4982 (1987).